

Study of Phase Stability and Negative Permittivity Behaviour of Undoped and Doped Sr_2MnO_4

Submitted in partial fulfilment for the award of degree
DOCTOR OF PHILOSOPHY

by

Gurudeo Nirala

Under the Supervision of

Dr. Shail Upadhyay



Department of Physics
Indian Institute of Technology
(Banaras Hindu University)
Varanasi

Roll No. 17171012

August 2022



Certificate

It is certified that the work contained in the thesis entitled “*Study of Phase Stability and Negative Permittivity Behaviour of Undoped and Doped Sr_2MnO_4* ” by Mr. Gurudeo Nirala (Roll No. 17171012), in partial fulfillment of the requirement for award of degree of **Doctor of Philosophy** at **Indian Institute of Technology (BHU), Varanasi**, is a record of his own work carried out under my supervision and guidance and that this work has not been submitted elsewhere for an award of any other degree anywhere unless explicitly referenced.

It is further certified that the student has fulfilled all the requirements of Comprehensive Examination, Candidacy and SOTA for the award of Ph.D. Degree.

(supervisor)

Dr. Shail Upadhyay

Associate Professor

Department of Physics

Indian Institute of Technology

(Banaras Hindu University)

Varanasi (U.P.)-221005.



भारतीय
प्रौद्योगिकी
संस्थान
बनारस हिन्दू विश्वविद्यालय



INDIAN
INSTITUTE OF
TECHNOLOGY
BANARAS HINDU UNIVERSITY

Certificate

It is certified that the work contained in the thesis entitled "*Study of Phase Stability and Negative Permittivity Behaviour of Undoped and Doped Sr_2MnO_4* " by Mr. Gurudeo Nirala (Roll No. 17171012), in partial fulfillment of the requirement for award of degree of Doctor of Philosophy at Indian Institute of Technology (BHU), Varanasi, is a record of his own work carried out under my supervision and guidance and that this work has not been submitted elsewhere for an award of any other degree anywhere unless explicitly referenced.

It is further certified that the student has fulfilled all the requirements of Comprehensive Examination, Candidacy and SOTA for the award of Ph.D. Degree.


Associate Professor
Department of Physics
Indian Institute of Technology
Banaras Hindu University
Varanasi-221005

Department of Physics
Indian Institute of Technology
(Banaras Hindu University)
Varanasi (U.P.)-221005.



भारतीय
प्रौद्योगिकी
संस्थान
काशी हिन्दू विश्वविद्यालय



INDIAN
INSTITUTE OF
TECHNOLOGY
BANARAS HINDU UNIVERSITY

Declarations by the Candidate

I, **Gurudeo Nirala** (Roll No. 17171012), certify that the work embodied in this thesis is my own bonafide work and carried out by me under the supervision of *Dr. Shail Upadhyay* from 2017 to 2022, at the Department of Physics, Indian Institute of Technology (BHU), Varanasi. The matter embodied in this thesis has not been submitted for the award of any other degree/diploma. I declare that, I have faithfully acknowledged and given credits to the research workers wherever their works have been cited in my work in this thesis. I further declare that, I have not willfully copied from any other's work, paragraphs, text, data, results, *etc.*, reported in journals, books, magazines, reports dissertations, theses, *etc.*, or available at websites and have not included them in this thesis and have not cited as my own work.

Date: -

Gurudeo Nirala

Place: -

(17171012)

Certificate by the Supervisor

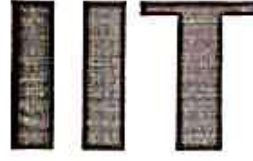
It is certified that the above statement made by the student is correct to the best of our knowledge.

Supervisor
(Dr. Shail Upadhyay)

Head of Department



भारतीय
प्रौद्योगिकी
संस्थान
काशी हिन्दू विश्वविद्यालय



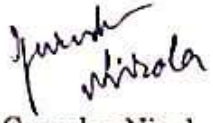
INDIAN
INSTITUTE OF
TECHNOLOGY
BANARAS HINDU UNIVERSITY

Declarations by the Candidate

I, **Gurudeo Nirala** (Roll No. 17171012), certify that the work embodied in this thesis is my own bonafide work and carried out by me under the supervision of *Dr. Shail Upadhyay* from 2017 to 2022, at the Department of Physics, Indian Institute of Technology (BHU), Varanasi. The matter embodied in this thesis has not been submitted for the award of any other degree/diploma. I declare that, I have faithfully acknowledged and given credits to the research workers wherever their works have been cited in my work in this thesis. I further declare that, I have not willfully copied from any other's work, paragraphs, text, data, results, etc., reported in journals, books, magazines, reports dissertations, theses, etc., or available at websites and have not included them in this thesis and have not cited as my own work.

Date: - 18/08/22

Place: - Varanasi


Gurudeo Nirala

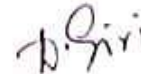
(17171012)

Certificate by the Supervisor

It is certified that the above statement made by the student is correct to the best of our knowledge.



Supervisor
(Dr. Shail Upadhyay)
Associate Professor
Department of Physics
Indian Institute of Technology
(Banaras Hindu University)
Varanasi-221005



Head of Department
HEAD/विभागाध्यक्ष
भौतिक विभाग/Deptt. of Physic.
काशी-221005/(अवहिताश्रम)/IIT (BHU)
वाराणसी/Varanasi-221005



भारतीय
प्रौद्योगिकी
संस्थान
काशी हिन्दू विश्वविद्यालय



INDIAN
INSTITUTE OF
TECHNOLOGY
BANARAS HINDU UNIVERSITY

Copyright Transfer Certificate

**Title of the Thesis: Study of Phase Stability and Negative Permittivity
Behaviour of Undoped and Doped Sr_2MnO_4 .**

Name of the Student: Gurudeo Nirala

Copyright Transfer

The undersigned hereby assigns to the Indian Institute of Technology (Banaras Hindu University) Varanasi all rights under copyright that may exist in and for the above thesis submitted for the award of the “*Doctor of Philosophy*”.

Date: -

Gurudeo Nirala

Place: -

(17171012)

Note: However, the author may reproduce or authorize others to reproduce material extracted verbatim from the thesis or derivative of the thesis for author's personal use provided that the source and the Institute's copyright notice are indicated.



भारतीय
प्रौद्योगिकी
संस्थान
काशी हिन्दू विश्वविद्यालय



INDIAN
INSTITUTE OF
TECHNOLOGY
BANARAS HINDU UNIVERSITY

Copyright Transfer Certificate

Title of the Thesis: Study of Phase Stability and Negative Permittivity
Behaviour of Undoped and Doped Sr_2MnO_4 .

Name of the Student: Gurudeo Nirala

Copyright Transfer

The undersigned hereby assigns to the Indian Institute of Technology (Banaras Hindu University) Varanasi all rights under copyright that may exist in and for the above thesis submitted for the award of the "Doctor of Philosophy".

Date: - 18/08/22

Place: - Varanasi


Gurudeo Nirala

(17171012)

Note: However, the author may reproduce or authorize others to reproduce material extracted verbatim from the thesis or derivative of the thesis for author's personal use provided that the source and the Institute's copyright notice are indicated.

Acknowledgements

I express my sincere gratitude and indebtedness to my research supervisor *Dr. Shail Upadhyay*, Associate Professor, Department of Physics, Indian Institute of Technology (Banaras Hindu University) for her valuable guidance, encouragement and help throughout the tenure of this research work. I am incredibly grateful to her for her keen interest in the investigation and the academic support. In the course time, she motivated, inspired and extended the necessary educational assistance in carrying out my research work. In spite of her busy schedule, she participated in each minute details of my progress of work and shared my pleasures and anxieties as well on the research findings.

I am grateful to my RPEC members, *Dr. Swapnil Patil* Department of Physics, and *Dr. Ashutosh Kumar Dubey*, Department of Ceramic Engineering, Indian Institute of Technology (Banaras Hindu University) for their guidance. In the entire research tenure, their valuable discussions and encouragement helped this journey to a fruitful end.

I am immensely rejoiced to owe my deep sense of gratitude to *Prof. B. N. Dwivedi*, *Prof. D. Giri*, *Prof. P. Singh*, *Prof. R. Prasad*, *Dr. P. C. Pandey*, *Dr. A. Mohan*, *Dr. S. Tripathi* and *Dr. S. Singh* for their constant encouragement during research work. I am thankful to, *Prof. S. Chatterjee*, Head, Department of Physics, for providing me all the facilities available in the department during my research work.

I am grateful to the Coordinator, Central Instrument Facility Center (CIFC), IIT (BHU), Varanasi for providing the experimental facilities required for the characterization of the synthesized samples.

I am also thankful to all non-teaching staff of the Department of Physics for their kind cooperation. I wish to express my sincere gratitude to all those who have extended their helping hands in various ways during my tenure at Indian Institute of Technology (Banaras Hindu University), Varanasi, India.

In the last but not least I am very thankful to my lab mate and friends – Dr. Upendra Kumar, Dr. Dharmendra Yadav, Tarun Katheriya, Dr. Prince Gupta, Balveer Singh, Dipti Arya, Vaibhav Chauhan, Digvijay Nath Dubey, Prashant Pandey, Prashant Dixit, Raj Kumar, Vivek Semwal, Mohd. Alam, Md. Bayzeed Alam, Abhishek Kumar Singh, Rohit Kumar Shukla, and Harish Verma for providing company during the Ph.D. research work.

Date: -

Gurudeo Nirala

Place: -

In the last but not least I am very thankful to my lab mate and friends – Dr. Upendra Kumar, Dr. Dharmendra Yadav, Tarun Katheriya, Dr. Prince Gupta, Balveer Singh, Dipti Arya, Vaibhav Chauhan, Digvijay Nath Dubey, Prashant Pandey, Prashant Dixit, Raj Kumar, Vivek Semwal, Mohd. Alam, Md. Bayzeed Alam, Abhishek Kumar Singh, Rohit Kumar Shukla, and Harish Verma for providing company during the Ph.D. research work.

Date: - 18/08/22

Place: - Varanasi


Gurudeo Nirala

Dedicated to my family and friends...

Table of Contents

CERTIFICATE	III
DECLARATIONS BY THE CANDIDATE	V
CERTIFICATE BY THE SUPERVISOR	V
COPYRIGHT TRANSFER CERTIFICATE	VII
ACKNOWLEDGEMENTS	IX
TABLE OF CONTENTS	XIII
LIST OF FIGURES	XVII
LIST OF TABLES	XXI
PREFACE	XXIII
CHAPTER 1 INTRODUCTION	1-1
1.1 PEROVSKITES: STRUCTURAL DIVERSITY.....	1-3
1.2 RUDDLESDEN D POPPER (RP) OXIDE PHASE	1-6
1.2.1 <i>Crystal Structure</i>	1-9
1.2.2 <i>Oxygen Stoichiometry and Carrier Concentration</i>	1-12
1.2.3 <i>Electrical Properties</i>	1-16
1.2.4 <i>Applications</i>	1-18
1.3 PERMITTIVITY (E) AND PERMEABILITY (M)	1-20
1.4 NEGATIVE PERMITTIVITY MATERIALS.....	1-21
1.4.1 <i>Metamaterials</i>	1-22
1.4.2 <i>Composites</i>	1-24
1.5 THEORETICAL MODELS.....	1-28
1.5.1 <i>Drude Model</i>	1-29
1.5.2 <i>Lorentz Oscillator Model</i>	1-30
1.5.3 <i>Drude-Lorentz model</i>	1-33
1.6 MOTIVATION OF THE WORK	1-34
CHAPTER 2 MATERIALS PREPARATION AND CHARACTERISATIONS	2-39
2.1 MATERIALS PREPARATION AND CHARACTERISATIONS	2-41

2.2	MATERIALS SYNTHESIS	2-42
2.2.1	<i>Selection of raw materials</i>	2-42
2.2.2	<i>Weighing of raw materials</i>	2-43
2.2.3	<i>Mixing of raw materials using ball mill</i>	2-43
2.2.4	<i>Calcination of Mixtures</i>	2-46
2.2.5	<i>Granulation or Palettization</i>	2-47
2.2.6	<i>Sintering of Pellets</i>	2-47
2.3	CHARACTERIZATION	2-48
2.3.1	<i>X-ray diffraction analysis</i>	2-48
2.3.2	<i>Field Emission Scanning Electron Microscope (FESEM)</i>	2-60
2.3.3	<i>Fourier Transform Infrared Spectroscopy (FTIR)</i>	2-62
2.3.4	<i>X-Ray Photoelectron Spectroscopy (XPS)</i>	2-63
2.3.5	<i>Ultra-Violet Visible Near Infra-Red (UV-Vis-NIR) Spectroscopy</i>	2-66
2.3.6	<i>Alternating Current (AC) Electrical data analysis</i>	2-68
CHAPTER 3 SYNTHESIS AND CHARACTERISATION OF SR_2MNO_4		3-71
3.1	INTRODUCTION	3-73
3.2	EXPERIMENTAL.....	3-74
3.3	RESULTS AND DISCUSSIONS.....	3-75
3.3.1	<i>Phase Analysis and Structural Characterization</i>	3-76
3.3.2	<i>FTIR Spectroscopic Studies</i>	3-81
3.3.3	<i>Microstructural Studies</i>	3-82
3.3.4	<i>UV-Visible Spectroscopic Studies</i>	3-83
3.3.5	<i>XPS Analysis</i>	3-85
3.4	ELECTRICAL STUDIES	3-86
3.4.1	<i>AC conductivity</i>	3-86
3.4.2	<i>Modulus and Impedance Spectroscopic Analysis</i>	3-96
3.5	CONCLUSIONS.....	3-97
CHAPTER 4 SYNTHESIS AND CHARACTERISATION OF $\text{LA}_x\text{SR}_{2-x}\text{MNO}_4$.....		4-99
4.1	INTRODUCTION	4-101
4.2	EXPERIMENTAL.....	4-103
4.3	RESULTS AND DISCUSSION.....	4-104
4.3.1	<i>Crystal Structure</i>	4-104

4.3.2	<i>Microstructural characterization</i>	4-110
4.3.3	<i>X-Ray Photoelectron Spectroscopy Analysis</i>	4-111
4.3.4	<i>Negative Permittivity Behaviour</i>	4-113
4.4	CONCLUSIONS.....	4-121
CHAPTER 5 SYNTHESIS AND CHARACTERISATION OF $SR_2MN_{1-x}SN_xO_4$....		5-123
5.1	INTRODUCTION	5-125
5.2	EXPERIMENTAL.....	5-127
5.3	RESULTS AND DISCUSSION.....	5-128
5.3.1	<i>Phase and Crystal structure analysis</i>	5-128
5.3.2	<i>Microstructural characterization</i>	5-132
5.3.3	<i>Negative Permittivity</i>	5-134
5.3.4	<i>XPS Analysis</i>	5-141
5.3.5	<i>UV-Vis-NIR Spectroscopy</i>	5-144
5.4	CONCLUSIONS.....	5-146
CHAPTER 6 SYNTHESIS AND CHARACTERISATION OF $SR_2MN_{1-x}NB_xO_4$...		6-147
6.1	INTRODUCTION	6-149
6.2	EXPERIMENTAL.....	6-151
6.3	RESULTS AND DISCUSSION.....	6-152
6.3.1	<i>Phase analysis and Crystal structure</i>	6-152
6.3.2	<i>Microstructural characterization</i>	6-158
6.3.3	<i>X-Ray Photoelectron Spectroscopy Analysis</i>	6-158
6.3.4	<i>Negative Permittivity</i>	6-161
6.4	CONCLUSIONS.....	6-170
CHAPTER 7 CONCLUSIONS AND FUTURE SCOPE		7-173
7.1	SUMMARY AND CONCLUSIONS.....	7-175
7.2	FUTURE SCOPE.....	7-176
CHAPTER 8 BIBLIOGRAPHY		8-179

List of Figures

Figure 1.1. A unit cell of ABO_3 type cubic perovskite oxide structure.	1-3
Figure 1.2. Schematic crystal structures of $n = 1, 2$ and 3 members of Ruddlesden–Popper type $A_{n+1}B_nO_{3n+1}$ [8].....	1-6
Figure 1.3. Ideal tetragonal unit cell of stoichiometric A_2BO_4 layered perovskite crystalized in $I4/mmm$ space group.....	1-7
Figure 1.4. (a) Half unit cell of T-type La_2NiO_4 layered perovskite. (b) Unit cell of T'-type Pr_2CuO_4 ternary oxide.....	1-10
Figure 1.5. Schematic representation of location of oxygen vacancies and interstitial oxide ions in A_2BO_4 layered perovskite [66].	1-13
Figure 1.6. Classification of materials according to their permittivity (ϵ) and permeability (μ) [96].....	1-20
Figure 1.7. Schematic diagram of lattice of periodic metal wires proposed by J. B. Pendry [96].	1-23
Figure 2.1. Working Principle of Lab Planetary Ball-Miller.....	2-44
Figure 2.2. Flowchart of materials preparation.....	2-47
Figure 2.3. Schematic illustration of X-ray diffraction from a crystal.	2-49
Figure 2.4. Visualization of Bragg's law.	2-50
Figure 2.5. Schematic representation of $\theta/2\theta$ diffraction in Bragg-Brentano geometry.....	2-50
Figure 2.6. A typical FullProf software interface during Rietveld refinement process.	2-54
Figure 2.7. X-ray diffractometer (XRD) at Central Instrument Facility (CIF) IIT (BHU).	2-57
Figure 2.8. The Schematic view of a Field Emission Scanning Electron Microscope (FESEM).	2-61
Figure 2.9. FESEM facilities at Central Instrument Facility (CIF) IIT (BHU).	2-62
Figure 2.10. Principle of FT-IR spectroscopy and experimental set-up for FTIR measurement facility.	2-63
Figure 2.11. Schematic diagram of energy levels of sample and spectrometer. Note that the conducting specimen and spectrometer housing is in electrical contact [177].....	2-65
Figure 2.12. XPS Facility at Central Instrument Facility (CIF) IIT (BHU).	2-66
Figure 2.13. Experimental Set-up for UV-Vis.-NIR measurement (IIT BHU).	2-68
Figure 2.14. Experimental Set up for electrical measurements (IIT BHU).	2-68
Figure 3.1. Flow chart of the synthesis of powders and ceramics.	3-74

Figure 3.2. (a) XRD pattern of the samples, (b) Rietveld refinement of XRD data, and SSP plot (inset) of the sample SMQ (Sr_2MnO_4).....	3-76
Figure 3.3. FTIR spectra of samples SM4 and SMQ (Sr_2MnO_4).	3-81
Figure 3.4. SEM micrographs of a sintered pellet of samples.	3-82
Figure 3.5. (a) Tauc's plot for sample SMQ (Sr_2MnO_4). The UV-visible absorption spectrum is shown in the inset. (b) $\ln(\alpha)$ versus $h\nu$ plot for determining Urbach tail width.	3-84
Figure 3.6. XPS spectra of Mn 2p present in the sample SMQ (Sr_2MnO_4). Symbols represent the recorded spectrum and the solid line represents the fit and background.....	3-85
Figure 3.7. Conductivity spectra of the sample SMQ (Sr_2MnO_4) at different temperatures. Symbols represent the experimental data points and the solid lines represent the theoretical JPL fitting.....	3-87
Figure 3.8. Arrhenius representation of DC conductivity for sample SMQ (Sr_2MnO_4).....	3-90
Figure 3.9. Variation of frequency exponent n with temperature for the sample SMQ (Sr_2MnO_4).	3-92
Figure 3.10. Total conductivity of sample SMQ (Sr_2MnO_4) at different frequencies.	3-94
Figure 3.11. Ghosh scaling for the sample SMQ (Sr_2MnO_4).	3-95
Figure 3.12. Variation of M'' and Z'' with frequency $\log(f)$ at different temperatures for the sample SMQ (Sr_2MnO_4).	3-96
Figure 4.1. (a) Room temperature XRD pattern of the samples, (b, c, d, e) Rietveld refined XRD pattern of the samples (f) Variation of lattice parameters with La Concentration (x).	4-105
Figure 4.2. (a) SEM images of the fractured surfaces of the sintered pellets (b) Histograms showing the distribution of grain size in the samples.	4-110
Figure 4.3. Core-level XPS spectra of Mn 2p.....	4-112
Figure 4.4. Variation of the real part of the relative permittivity with frequency at a few selected temperatures.	4-113
Figure 4.5. Variation of fitting parameters (ω_{pd} , ω_{pl} , ω_d , γ) with temperature.....	4-116
Figure 4.6. AC conductivity spectra of the samples at some representative temperatures.	4-117
Figure 4.7. Variation of admittance with angular frequency at few selected temperatures.....	4-118
Figure 4.8. Optimum equivalent circuit.	4-118
Figure 4.9. Variation in the values of equivalent circuit elements (R_1 , R_2 , L_1 , L_2) with temperature.	4-120

Figure 5.1. (a) Room temperature XRD pattern of the samples, (b, c, d e) Rietveld refined XRD pattern of the samples (f) Variation of lattice parameters with Sn Concentration (x).....	5-129
Figure 5.2. (a) SEM images of the fractured surfaces of the sintered pellets (b) Histograms showing the distribution of grain size in the samples.	5-132
Figure 5.3. Temperature dependence of the real part of the relative permittivity at few representative frequencies.....	5-134
Figure 5.4. Variation of the real part of the relative permittivity with frequency at few selected temperatures.	5-136
Figure 5.5. AC conductivity spectra of the samples at some representative temperatures.	5-138
Figure 5.6. Variation of DC conductivity with increasing temperature and Sn Concentration (x).....	5-141
Figure 5.7. Core-level XPS spectra of Mn 2p and Sn 3d. Symbols represent the recorded spectrum and the solid line represents the fit and background.	5-142
Figure 5.8. UV-Vis-IR absorption spectra of the samples.....	5-145
Figure 6.1. (a) Room temperature XRD pattern of the samples, (b, c, d, e) Rietveld refined XRD pattern of the samples (f) Variation of lattice parameters with Nb Concentration (x).	6-154
Figure 6.2. SEM images of the fractured surfaces of the sintered pellets.	6-158
Figure 6.3. Core-level XPS spectra of Mn 2p and Nb 3d.	6-161
Figure 6.4. Temperature dependence of the real part of the relative permittivity (a-e) and dissipation factor (f-j) at few representative frequencies.....	6-163
Figure 6.5. Variation of the real part of the relative permittivity with frequency at a few selected temperatures.	6-164
Figure 6.6. Variation of DC conductivity with the inverse of temperature.	6-166
Figure 6.7. AC conductivity spectra of the samples at some representative temperatures.	6-168

List of Tables

Table 1.1. Tolerance factor of different crystal structure.	1-5
Table 1.2 Synthesized compositions, Sample Codes and Important investigation properties.....	1-37
Table 2.1 Specification of materials used in synthesis.	2-42
Table 3.1. Effect of cooling rate on the percentage (%) of two major phases in the synthesized powders.	3-77
Table 3.2. Structural parameters and reliability factors for sample SMQ (Sr_2MnO_4) obtained by Rietveld refinement of the XRD patterns.	3-80
Table 4.1. Structural parameters and reliability factors obtained by Rietveld refinement of the XRD patterns.	4-109
Table 4.2. XPS core level binding energy of Mn 2p and Nb 3d.....	4-112
Table 5.1. Structural parameters and reliability factors obtained by Rietveld refinement of the XRD patterns.	5-131
Table 5.2. XPS core level binding energy of Mn 2p and Sn 3d.	5-144
Table 6.1. Structural parameters and reliability factors obtained by Rietveld refinement of the XRD patterns.	6-157
Table 6.2. XPS core level binding energy of Mn 2p and Nb 3d.....	6-160

Preface

Permittivity and permeability are two fundamental physical properties of materials that describe how they react to electromagnetic, magnetic and electric fields. Materials are divided into four quadrants based on the permittivity (epsilon, ϵ) and permeability (mu, μ) sign. These include common materials (both ϵ and μ are positive), double-negative materials, mu-negative materials, and epsilon-negative materials. The incident electromagnetic waves are transparent to common materials with positive permittivity and permeability, and the electric vector (**E**), magnetic vector (**B**), and wave vector (**k**) correspond to the right-handed rule. Electromagnetic waves can propagate within materials having double negative characteristics, such as metamaterials, but the relationships between **E**, **B**, and **k** are left-handed. In materials with solely negative permittivity or negative permeability, electromagnetic waves fade evanescently. Epsilon-negative materials were initially realised in metamaterials, while mu-negative characteristics were first obtained in ferrites at their magnetic resonance frequency. In recent years, the material having negative permittivity (ϵ) or/and permeability (μ) have been extensively explored due to their potential applications in optical filters, medical devices, remote aerospace applications, sensor detection, infrastructure monitoring, smart solar power management, crowd control, radoms, high-frequency battlefield communication, lenses for high-gain antennas, improving ultrasonic sensors, and even shielding structures from earthquakes, etc.

The negative permittivity is essential for the meta-performance like negative refraction, negative phase velocity, reverse Doppler effect and Cerenkov effect, etc. Negative permittivity materials have shown great potential in various electromagnetic and electronic applications, such as electromagnetic shielding, wave absorbing, laminated capacitors, and coil-less inductors. The concept of negative permittivity is not new. The permittivity of common metals

is always negative when the frequency is below their plasma frequency, ω_p , i.e., all metals below their plasma frequency are negative permittivity materials on their own. However, as frequency falls, the real part of permittivity rapidly declines while the imaginary part substantially increases. As a result, all metals lose their utility as negative permittivity materials in various applications. According to investigations conducted from the standpoint of materials science the negative permittivity can be realised in the radio-frequency band, which is significantly lower than the optical frequency.

In the beginning the concept for achieving/obtaining negative permittivity (ϵ) or/and permeability (μ) in radio frequency region was solely theoretical. Later it was realised in artificially designed/composed metamaterials, which consists artificially composed periodic arrays of metallic units, rarely seen in natural materials. The recent studies towards the development of metamaterials and realization of negative permittivity (ϵ) or/and permeability (μ) in natural materials highlighted the necessity of percolating metallic/conducting pathways in ceramic- or polymer-matrix composite(s). The critical percolating structures of building blocks brings challenges for composites to achieve microscopic (at atomic/molecular) level homogeneity that is needed to be used as coatings, film, or even other lower-dimensional materials or devices. This challenge can be overcome by realizing negative permittivity in mono-phase materials which is desirable for the miniaturization of the devices.

Finding a single-phase material showing negative permittivity is a challenging task and very few reports were available. Further, it is reported that negative permittivity depends on external parameters such as frequency and magnitude of the field and temperature. In most of the studies, negative permittivity has been studied as a function of the frequency and magnitude of an applied electric field. Study of negative permittivity as a function of temperature has rarely been made.

From the extensive literature survey, we have come to know that the single-phase materials which have shown negative permittivity in kHz to MHz frequency range are transition metals-based perovskite oxides (ABO_3) such as $PrMnO_3$, $LaSrMnO_3$, $LaCoEuTiO_3$, $LaFeO_3$, $GdFeO_3$, and $LaBaCoO_3$. Except La_2NiO_4 , no other system having general A_2BO_4 (Layered Perovskites or Ruddlesden-Popper) has been reported as negative permittivity material. The A_2BO_4 oxide is a two-dimensional perovskite like layer structure, in this structure it is easy to implant ions as dopants into the host lattice and hence manipulate its physical and chemical properties. In Sr_2MnO_4 multivalency of Mn cation offers the opportunity to tune its oxidation state via optimum dopant and its concentration, which may change electrical properties further.

The study of phase diagram of system Sr-Mn-O has shown that Sr_2MnO_4 is a metastable compound, it is stable only between 1350 °C to 1680 °C. Therefore, synthesis of pure Sr_2MnO_4 and its stabilization at low temperature (below 1350 °C) is a challenging task. Attempts have been made to synthesize compositions of La doped $La_xSr_{2-x}MnO_4$, but only synthesis of the compositions in the range $0.25 \leq x \leq 0.7$ could be possible. Therefore, in the view of above-mentioned challenges and to explore the possibility of Sr_2MnO_4 as negative permittivity material, in this thesis work efforts have been made to synthesize doped Sr_2MnO_4 and study phase stability and negative dielectric properties using solid state ceramic route. To tailor observed negative dielectric properties, a few compositions of La (at Sr), Sn (at Mn) and Nb (at Mn) systems for the first time have been synthesized by the same procedure. The effect of selected dopants on phase stability, structure, microstructure and negative permittivity behaviour are studied in detail. Further, it is worth mentioning here that to study explicitly role of the dopant, processing parameters (calcination and sintering temperature and time) were kept same for all the samples. For convenience the introduction to the subject, experimental tools and carried out work in this thesis is presented in theses following seven chapters:

Chapter 1: This chapter briefly presents the introduction of perovskite and layered perovskite oxides. It also describes the scientific and technical investigations carried out on layered perovskite oxides. Various technological applications of A_2BO_4 oxides have also been briefly reviewed in this chapter. The effect of dopants on crystal structure, oxygen stoichiometry and effective carrier concentration are discussed. It is then followed by a brief history towards the development of negative permittivity materials, introduction to negative permittivity & current negative permittivity materials, their concurrent challenges, theoretical models explaining negative permittivity and motivation of work.

Chapter 2: This chapter describes the experimental procedure and techniques used for the preparation & characterization of the samples. The solid-state ceramic route is used for preparation of these materials and described with the help of a flow chart. The physics and methodology of experimental techniques used for characterising synthesized compositions has also been reviewed briefly.

Chapter 3: This chapter presents, the successful synthesis of Sr_2MnO_4 using the solid-state reaction technique. Quenching in air from 1500°C to room temperature yielded the pure phase powder of Sr_2MnO_4 . The purity of synthesized powder was further examined by FTIR analysis. The Rietveld refinement of XRD data confirmed the tetragonal structure and $I4/mmm$ space group. The band gap, computed from the Tauc's plot, was found to be 1.15 eV. The XPS analysis depicted the presence of Mn^{3+} and Mn^{4+} valence states. Measurement of the AC electrical conductivity over wide temperature ($30\text{-}500^\circ\text{C}$) and frequency ($0.020 - 2$ MHz) ranges were carried out. The conduction mechanism changed from small polaron tunnelling ($< 270^\circ\text{C}$) to non-overlapping large polaron tunnelling ($>270^\circ\text{C}$). The frequency versus imaginary part of the impedance (Z'') and modulus (M'') plots exhibited a change in the conduction domain with increase in temperature. This result was further verified by the Ghosh's scaling of the conductivity spectra.

Chapter 4: This chapter presents, the synthesis of few compositions of La doped $\text{La}_x\text{Sr}_{2-x}\text{MnO}_4$ ($x = 0.3, 0.5, 0.7$) system in the air using solid-state ceramic route. Permittivity and AC conductivity studies with respect to frequency and temperature exhibited negative permittivity in the entire range of the measurement (30-300 °C) at all measuring frequency (1 kHz - 2 MHz). The negative permittivity was analysed by the Drude-Lorentz model. It was found that negative permittivity is caused by the plasma oscillations of free charge carriers. The inductive characteristics of the samples has been studied by the modelling of impedance data using various combinations of resistors and inductors. The inductive character of samples shows the prospect of developing synthesized compositions as coil-less inductor.

Chapter 5: This chapter presents, the synthesis of few compositions of the system $\text{Sr}_2\text{Mn}_{1-x}\text{Sn}_x\text{O}_4$ ($x=0.0, 0.3, 0.5$) system in the air using solid-state ceramic route. A change in the sign (positive to negative) of the permittivity above a particular temperature (T_c) is observed at all the measured frequencies. The negative permittivity was analysed by the Drude-Lorentz model. It was found that negative permittivity is caused by the plasma oscillations of thermally excited free charge carriers. Analysis of XPS spectra confirmed the presence of mixed-valence states of both Mn (Mn^{4+} and Mn^{3+}) and Sn (Sn^{4+} and Sn^{2+}) ions. The UV-Vis.-IR spectroscopy results indicated generation of a large number of defect states in the forbidden bandgap region of Sr_2MnO_4 on the substitution of Sn at Mn site. Synthesized samples are promising metamaterials for radio frequency (10 Hz -2 MHz) region applications due to the high-temperature plasmonic behaviour.

Chapter 6: This chapter presents, the synthesis of few compositions of Nb doped $\text{Sr}_2\text{Mn}_{1-x}\text{Nb}_x\text{O}_4$ ($x = 0.1, 0.2, 0.3, 0.4, 0.5$) system in the air using solid-state ceramic route. Out of these, the $x=0.4, 0.5$ compositions were found to consist of an impurity of $\text{Sr}_8\text{Nb}_4\text{O}_{18}$, which elucidates a solubility limit of Nb in the Sr_2MnO_4 . Permittivity and AC conductivity studies with respect to frequency and temperature exhibited negative permittivity in the entire range

of the measurement (30-600 °C) for $x = 0.1, 0.2$ compositions, whereas in the case of $x=0.3, 0.4,$ and 0.5 compositions, the same behaviour was seen above 80°C, 180°C, and 230°C, respectively. The plasmonic oscillations of charge carriers may be responsible for the negative permittivity behaviour, which is analysed by the Drude-Lorentz model. Compositional and temperature dependent sign of the permittivity of the system $\text{Sr}_2\text{Mn}_{1-x}\text{Nb}_x\text{O}_4$ makes this system promising materials for switching action in the wide frequency range and temperature range.

Chapter 7: This chapter sums up the overall conclusions of the investigations carried out in the thesis work. A few important suggestions for future scope are also mentioned in this chapter.